Check for updates

Injectable sustained-release hydrogel for high-concentration antibody delivery†

Talia Zheng [ID] and Patrick S. Doyle [ID] *

There is an increasing interest in subcutaneous (SC) delivery as an alternative to the traditional intravenous (IV) for immunotherapies and other advanced therapies. High-concentration formulations of antibodies are needed to meet the limited-volume requirements of subcutaneous SC delivery. Despite this need, there remain challenges in delivering stable and injectable antibodies in these high concentrations. Hydrogel encapsulation of amorphous solid antibodies has been proven to improve the stability and injectability of high-concentration antibody formulations. However, the antibody is quickly released from the hydrogel due to the material's porosity, leading to rapid, uncontrolled drug release kinetics undesirable for the drug's efficacy and safety. In this paper, we propose a dual-network composite hydrogel which leverages interactions between the two polymer networks to achieve controlled release of the antibody. We load the solid form of the antibody at high concentrations within alginate hydrogel microparticles which are then suspended in thermogelling methylcellulose solution to formulate the *in situ* gelling composite hydrogel. By facile chemical modification of the alginate to tune the microparticles' gel properties and alginate–methylcellulose interactions, we demonstrate how the composite system can delay release of the drug in a tunable manner and achieve a near-zero order release profile for improved therapeutic efficacy. We show acceptable injectability properties of the composite hydrogel at high antibody concentrations, highlighting the functionalities of dualnetwork encapsulation. We imagine this composite system to be applicable for the sustained delivery of various therapeutic protein forms, especially for high-loading SC formulations.

Introduction

In the last decade, there have been several advances in the treatment of cancer and auto-immune diseases through the administration of biologics, specifically antibody drugs.[1,2] These antibodies are often formulated as liquids at low concentrations and injected intravenously; however, IV infusions require hospital/clinic care and are burdensome for both patients and providers.[3,4] Subcutaneous (SC) injection is a more preferred delivery format and can also enable self-administration and home-based care.[4–6] In SC delivery, the total injection volume is limited (typically 2 mL or less), necessitating high-concentration antibody solutions (>100 mg mL^{-1}). But such solutions are extremely viscous due to self-association among the antibodies, and therefore challenging to process and deliver.[7,8] SC delivery as an alternative to IV has been emerging as part of the paradigm shift towards patient-centric clinical practice and out-of-clinic care, making high-

concentration antibody formulations a salient need for current and future developments in the therapeutic landscape.[9,10] Previous work has circumvented the issues of high viscosity and instability by formulating antibodies as amorphous solid dispersions (ASDs), which can be packed to high concentrations.[11] Further, the antibody ASDs are encapsulated in alginate microparticles, which are biocompatible, shear-thinning materials that allow the solid antibodies to be easily injected. With this approach, our group has been able to formulate stable, high-concentration protein suspensions, fulfilling the need for SC-injectable antibody formulations. While this approach is promising, the permeability and fast swelling of the alginate hydrogel mesh leads to burst release of the antibody, which can reduce the dosage efficacy as well as potentially lead to systemic side effects.[12] These effects are especially pronounced at high concentrations, as hydrogels typically lead to more significant burst release in the case of high drug loadings.[13,14] Therefore, there is a need to develop high-concentration antibody formulations that enable more consistent and sustained delivery, which are preferred for long-term efficacy and ease of use.[15,16]

Thermoresponsive polymers are commonly used to achieved sustained release in hydrogel drug delivery systems and have been previously investigated for SC-injectable

Department of Chemical Engineering, 400 Main Street, Cambridge, MA 02139, USA.
E-mail: pdoyle@mit.edu

†Electronic supplementary information (ESI) available: Chemical modification scheme, injectability testing set-up, and measurement of antibody solubility. See DOI: https://doi.org/10.1039/d4pm00290c

biologics.[17,18] These polymers are liquid in solution at room temperature and gel at body temperature, thus slowing diffusion from and erosion of the hydrogel. Composite hydrogels have also been investigated for sustained-release of biologics. For example, polymer micro- or nanoparticles may be embedded within a thermo-gelling matrix that eliminates the burst release from the particles alone.[19,20] Notably, current injectable formulations in these systems have been limited to low drug concentrations (<1–50 mg mL^{-1}).[14,21–24] Methylcellulose (MC) is a thermoresponsive polysaccharide which has been employed for suppressing burst release due to its ability to form a depot at body temperature and has been shown to be biocompatible and non-toxic in the SC environment.[18,25–27] Its thermoresponsive behavior has been well-studied, and previous studies have proposed that the increase in temperature causes fibril formation as well as the association of hydrophobic domains leading rise to the gel network structure.[28–30] Methylcellulose is also known to form semi-interpenetrating networks with alginate, due to MC's ability to thermally gel through hydrophobic associations and alginate's native ionic cross-linking as well as hydrogen bonding between the two networks.[31–33] In this work, we combine antibody-laden alginate microparticles with a methylcellulose thermogel to suppress burst release and instead enable sustained release from the particles while maintaining the advantages of hydrogel encapsulation of the highly concentrated antibodies, such as injectability. The inter-network polymer interactions can be specifically tuned through chemical modification of alginate to tune the release behavior of the composite hydrogel.

The aim of this work is to develop a high-concentration, injectable antibody formulation which has a sustained release profile. Our formulation consists of antibody ASD-laden alginate microparticles suspended in a methycellulose polymer solution. Upon injection (and hence reaching body temperature), the system thermally associates *in situ* to form a composite dual-network system. This associated network both reduces burst release and enables sustained release of highly concentrated antibody drugs achieved through a simple and gentle formulation process. We integrate the ease of formulation and desirable flow properties of hydrogel encapsulation in alginate microparticles with the sustained-release capabilities of thermogelling methylcellulose to form a novel dosage form for antibodies. The work described here builds upon our previous work on formulating highly concentrated antibodies by enabling controlled- and sustained-release with our hydrogel encapsulation platform, which can be generalized to multiple antibodies and forms (amorphous or crystalline).[11,34]

Experimental methods

Materials

All chemicals used were of analytical grade. Sodium alginate (viscosity 5–40 cP) and methylcellulose (MC, viscosity 15 cP) were purchased from Sigma. Poly(ethylene glycol) (PEG,

3350 kDa) was purchased from Hampton Research. Lyophilized human IgG was purchased from Equitech-Bio, Inc. All other chemicals were purchased from Sigma and used without further purification.

Composite hydrogel formulation antibody precipitation

For preparation of amorphous solid dispersions (ASDs) of human total IgG, 500 μL of 40 mg mL^{-1} antibody in 50 mM HEPES (*N*-2-hydroxyethylpiperazine-*N*-2-ethane sulfonic acid) solution was mixed with 1000 μL of 25% w/v PEG in 50 mM HEPES solution. IgG was precipitated at pH 7.4. Precipitation was carried out in batches at a total volume of 1.5 mL, with each batch yielding 20 mg of the antibody. All solutions were prepared with distilled water and filtered with a 0.2 μm filter. The precipitation mixture was kept at room temperature for 4 h while rotating at 12 rpm on a tube mixer. Amorphous solid IgG were recovered by centrifugation at 1700 RCF for 30 minutes at 4 °C. For later evaluation of the ASDs, the solid antibodies were resuspended in 10% w/v PEG solution buffered with 50 mM HEPES pH 7.4 (storage buffer). ASDs containing MC were prepared by resuspending the solid antibodies in 4% w/v MC solution with 10% w/v PEG and HEPES buffer.

Alginate modification

For hydrophobic modification of the alginate polymer, sodium alginate was first oxidized and then further modified by reductive amination of the oxidized alginate. For preparation of the oxidized alginate (OA), sodium alginate was dissolved in DI water at 2% w/v. Sodium periodate was dissolved in DI water at 1.3 mg mL^{-1} (for 3 molar% uronic oxidation) and 2.6 mg mL^{-1} (for 6 molar% uronic oxidation). 50 mL of the sodium periodate solution was mixed with 100 mL of the sodium alginate solution to carry out the oxidation reaction at room temperature for 24 h in dark conditions while mixing. After, reaction byproducts and unreacted species were removed from the reaction mixture by dialysis with 3.5 kDa snakeskin dialysis tubes for 48 h. The product was concentrated using a 5 kDa centrifugal filter and freeze-dried. For preparation of the alkylated alginate, the freeze-dried oxidized alginate was dissolved in phosphate buffer (0.1 M, pH 7) at 2% w/v. Octylamine was added dropwise to the OA solution while stirring, with a molar ratio of octylamine to the oxidized uronic acid units of 5 : 1. The reducing agent, NaBH$_3$CN, was dissolved in a small amount of the same phosphate buffer and added to the reaction mixture, with a molar ratio of NaBH$_3$CN to octylamine of 1 : 1, following previously-reported schemes. NaBH$_3$CN was used as the reducing agent due to its higher selectivity and reactivity than other reducing agents, particularly at the neutral pH range.[35–37] The reaction was carried out at room temperature for 48 h in dark conditions while mixing. After, reaction byproducts and unreacted species were removed by dialysis as described above for 5 days. The final product was concentrated using a 5 kDa centrifugal filter, freeze-dried, and stored at 4 °C.

Antibody encapsulation

For preparation of the antibody pre-gel suspension, sodium alginate (2% w/v) was dissolved in 10% w/v PEG solution buffered with 50 mM HEPES at pH 7.4. For pre-gels containing MC, methylcellulose was dissolved with the alginate solution at 4% w/v. The resulting solution was filtered using a 0.2 μm filter. The PEG was used to stabilize the antibody precipitates in the amorphous solid state. The alginate solution was added to the solid antibody precipitates in excess and mixed to make a homogeneous suspension, then concentrated via centrifugation at 2500 RCF for 4 h at 4 °C. Excess supernatant was removed and the solid antibodies were resuspended in the remaining solution. To measure the protein concentration, the final pre-gel was diluted 20-fold in phosphate buffered saline (PBS) and measured in a Nanodrop UV-vis spectrophotometer using the 280 nm absorbance method.

For preparation of the antibody-laden particles, the pre-gel suspension (containing alginate) was filled inside a simple microfluidic device made from a plastic syringe barrel connected to a 30 gauge (ID = 159 μm, OD = 312 μm) blunt-tip needle. The crosslinking bath consisted of 40 mM CaCl$_2$, 10% w/v PEG, and 50 mM HEPES pH 7.4 and was filled inside a 50 mL centrifuge tube to form the collection bath. The distance from the tip of the needle dispenser to the bath was 3 mm. The device was centrifuged for 15–30 minutes at 400 RCF.

Antibody loading of the final formulations was measured as described above using the 280 nm absorbance method. Encapsulation efficiency of the hydrogel particles was evaluated by measuring the protein concentration in the CaCl$_2$ cross-linking bath after synthesizing the particles, and comparing to the total amount of antibody used in the pre-gel.

Rheological characterization

For characterization of the rheological behavior of methylcellulose and alginate solutions, a stress-controlled rheometer (DHR-3, TA Instruments) was used. An upper-cone geometry (diameter = 60 mm, cone angle = 1.004°, truncated gap = 29 μm) module was used. The solution sample was added to the lower Peltier plate, then the upper cone was lowered to the truncated gap height. To minimize surface effects between the sample and the geometry, mineral oil was used to cover the exposed edge of the cone. Water was added to the top of the cone and a solvent trap was used to minimize solvent evaporation from the sample. The sample was conditioned at 20 °C prior to each experiment, including a 60 s pre-shear at 10 rad per s and a 60 s equilibration. The temperature ramp experiments were performed from 20 °C to 40 °C, with a ramp rate of 2 °C min^{-1}, at a strain amplitude of 1% and a frequency of 1.6 Hz (10 rad per s).

Swelling ratio measurement

Swelling ratio of blank alginate hydrogel particles were measured after cross-linking in a calcium bath. The particles were prepared from a solution of 2% w/v alginate buffered at

pH 7.4 with 50 mM HEPES. The cross-linking bath used consisted of 40 mM CaCl$_2$ and 0.01% w/v Tween 80 surfactant. The particles were synthesized via centrifugal synthesis as described earlier and then rinsed and dried carefully with a tissue paper before weighing on an analytical balance. The particles were dried overnight in a vacuum oven and weighed again after drying. The swelling ratio, Q_s, was calculated using the following equation:

$$Q_s = \frac{w_s - w_d}{w_d} \qquad (1)$$

where w_s is the swollen weight of the particles and w_d is the dried weight of the particles. All measurements were performed with triplicate samples.

In vitro release assays

For evaluating release of the antibody from the hydrogel, 50 μL of the hydrogel sample was injected into the bottom of a 2 mL glass vial filled with 1.8 mL of pre-warmed (37 °C) simulated bodily fluid (SBF), which was prepared to mimic the ionic composition of the SC environment with both mono- and divalent ions, as from the literature, with 7.996 g L^{-1} sodium chloride, 0.350 g L^{-1} sodium bicarbonate, 0.224 g L^{-1} potassium chloride, 0.228 g L^{-1} potassium phosphate dibasic trihydrate, 0.305 g L^{-1} magnesium chloride hexahydrate, 0.278 g L^{-1} calcium chloride, 0.071 g L^{-1} sodium sulfate, 6.057 g L^{-1} tris (hydroxymethyl) aminomethane, and 40 mL L^{-1} of 1 M hydrochloric acid.[38] At set time intervals, 400 μL of the supernatant was removed and taken for measurement of protein concentration using the 280 nm UV-vis absorbance method, and the sampled volume was replaced with fresh SBF. Measurements were taken in triplicate.

Injectability tests

For evaluating the injectability of the formulations, a Zwick-Roell mechanical testing machine (model BTC-EXMACRO.001) was used. A 500 N full-scale load cell and compression test flat plate attachment were equipped to the machine. A clamp system was used to securely hold the formulation-loaded syringe (plastic, 1 mL, ID = 4.78 mm) in place during the test. A 24 gauge (ID = 311 μm, OD = 566 μm) Luer-lock needle was connected to the syringe. For each displacement-controlled experiment, a stroke distance of 30 mm was used, corresponding to a ~0.5 mL injection volume. The stroke speed of each experiment was set according to the desired flow rate of injection, and the force exerted to push the syringe plunger down was recorded over the stroke distance of the test. All injectability tests were conducted at ambient conditions.

Results and discussion

Composite hydrogel design

In this work, we developed dual-network antibody-laden composite hydrogels by incorporating ionotropic gelation of alginate to encapsulate highly concentrated antibodies with the
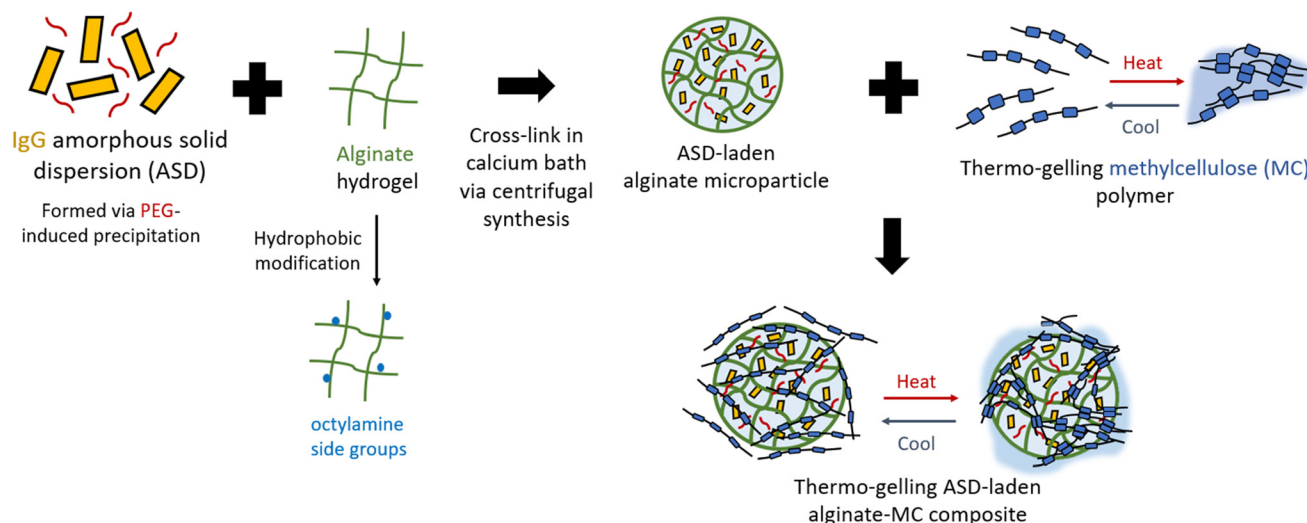
Fig. 1 Conceptual schematic of the proposed dual-network hydrogel design, compositing high-concentration antibody-loaded alginate microparticles with thermogelling methylcellulose polymer to result in a thermo-gelling composite hydrogel with complex inter-network interactions.

thermogelling capability of methylcellulose (MC). As illustrated in Fig. 1, we encapsulated amorphous solid immunoglobulin (IgG) antibodies, which are stabilized in the solid state using polyethylene glycol (PEG) into alginate hydrogel microparticles. The IgG ASD-laden microparticles were suspended in a solution of 4% w/v methylcellulose (MC). A second hydrogel network in this composite is formed *in situ* due to thermal gelation of MC upon injection. Here, human IgG was used as a model antibody drug because the majority of clinically-approved antibodies are IgG types.[39] We investigated interactions between the MC and alginate networks to tune the thermal gelation of the composite hydrogel towards sustained release of the antibody drug cargo. In addition to the native inter-network interpenetration and hydrogen bonding between alginate and MC, alginate was chemically modified through an oxidation-reductive amination (O-RA) route to graft a hydrophobic side group, octylamine, onto the alginate backbone. The O-RA route is a well-studied route for the preparation of hydrophobically-modified alginates, and unlike the amidation route, does not consume the polymer's carboxylate groups which are necessary for alginate cross-linking.[40–42] Following this route, alginate was first oxidized into a reactive aldehydic intermediate (2,3-dialdehydic alginate) and then underwent subsequent reductive amination, where octylamine was grafted at a degree of substitution of 3 or 6% to induce hydrophobic interactions between the alginate and MC hydrogels. A schematic of the reaction route is available in the ESI (Fig. S1†). Alginate was modified at relatively low degrees of substitution as oxidation of the polymer at degrees greater than 10% disrupts the backbone structure, resulting in reduction of alginate's cross-linking capability.[41,43]

Dual-network composite hydrogels, where polymer micro- or nanoparticles are embedded in another polymer matrix, have previously been used to achieve controlled release for protein drug delivery, but have so far been limited to low-concentration formulations (<100 mg mL^{-1}).[19,22,23,44,45] We present here a high-concentration (>100 mg mL^{-1}) formulation which meets dosage requirements for SC administration through a simple, modular formulation approach. We also tune specific polymer–polymer interactions within the composite hydrogel in order to access a range of drug release kinetics.

Composite hydrogel formulation and characterization

The microparticle formulation process was evaluated for particles synthesized with unmodified (0% d.s.) and modified (3% or 6% d.s.) alginates. Particles with IgG concentration of ~213 mg mL^{-1} were formed, which relates to the final formulation concentration (C_{form}) as

$$C_{form} = (\text{particle loading}) \times \varphi \qquad (2)$$

where φ is the effective particle volume fraction in suspension. The particle loading was measured by determining the volume of the antibody-laden particles and measuring the amount of encapsulated antibody in the particles. A C_{form} of 150 mg mL^{-1} was achieved with a particle volume fraction $\varphi = 0.70$ in the final formulation. The encapsulation efficiency (E.E.) of the particles was defined as the mass of encapsulated antibody over the total mass of antibody in the pre-gel. To measure the encapsulation efficiency, the antibody concentration in the pre-gel and the crosslinking bath were determined. The E.E. for all alginate formulations (Table S1, ESI†) varied between 98% and <100% w/w and is much higher than what is typically reported for proteins encapsulated in microspheres (60 to 75%).[44,46,47] In Fig. 2a, brightfield microscopy images of the IgG ASD-laden microparticles are shown, synthesized using 0, 3, or 6% substituted alginate (left to right), and the corresponding size distributions are shown below in Fig. 2b. A schematic of the microparticle synthesis process is available in the
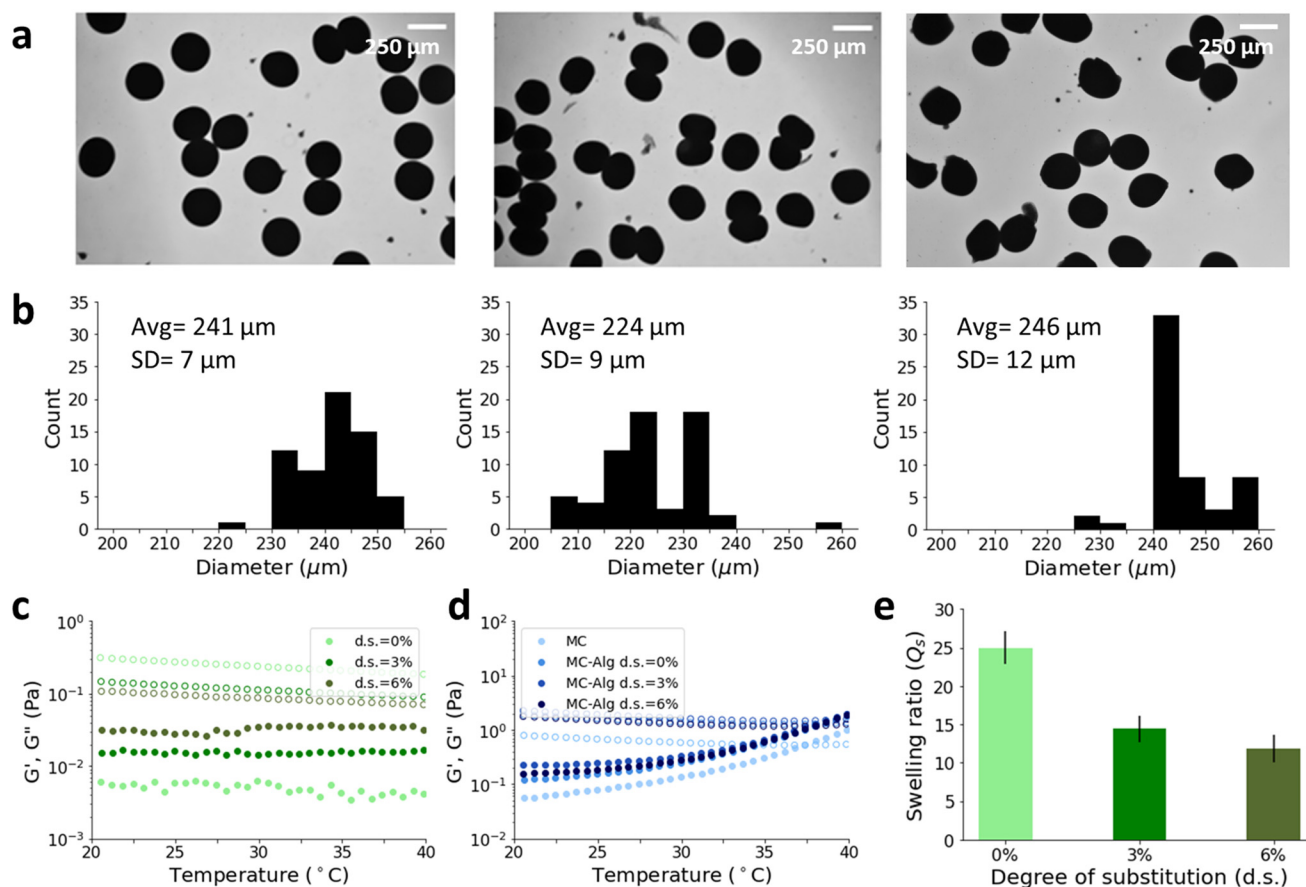
Fig. 2 (a) Brightfield microscopy images and (b) particle size distributions of synthesized antibody-loaded alginate microparticles with (left to right) 0%, 3%, and 6% degree of substitution. (c and d) Small amplitude oscillatory shear temperature sweep data for (c) 2% w/v alginate solutions with varying degree of substitution and (d) 4% w/v methylcellulose and 1% w/v alginate solutions with varying degree of substitution. (•) denotes storage modulus (G') and (∘) denotes loss modulus (G''). (e) Swelling ratio (Q_s) for blank (no ASD) alginate microparticles synthesized using 2% w/v alginate with varying degree of substitution.

ESI (Fig. S2†). The resulting particles are opaque due to the presence of the solid antibodies, which are stabilized with PEG. We show that the particle synthesis process is robust for modified alginates, indicating that the chemical modification does not affect alginate's ability to encapsulate antibodies, with similar controlled size distributions among all degrees of modification. Modification of the alginate provides an interesting way to modulate the delivery system's properties in a controllable manner, in particular to achieve sustained release. After the alginate microparticles were synthesized, they were suspended in a buffer containing 10% w/v PEG and 4% w/v MC. We show that the antibody remains in its solid form when methylcellulose is present in the buffer with PEG (Fig. S3, ESI†). In this process, particle synthesis and formation of the composite gel are independent of each other and thus enables modular changes to the formulation process. Importantly, we also show that the stability of the released antibody from the hydrogel is not affected in the formulation, either encapsulated in the alginate particle or in the composite hydrogel with methylcellulose, showing no significant change in the monomer percent compared to a control (Table S2, ESI†).

The rheological properties of hydrophobically-modified alginate with varying degrees of substitution were investigated, both alone and with methylcellulose in solution. In Fig. 2c, temperature sweep tests, used to measure the storage modulus (G') and loss modulus (G'') between 20–40 °C, for solutions of 2% w/v alginate polymer are shown. As expected, gelation and thermoresponsive behavior were absent in the unmodified and modified alginates, as $G' < G''$ over the entire temperature range shown. However, we observe a temperature-dependent increase and decrease in the storage and loss moduli, respectively, for the 3%- and 6%-substituted alginate solutions, which is not observed in the case of the unmodified alginate solution. As hydrophobic interactions increase in strength with temperature, the observed increase in storage modulus (elasticity) with respect to temperature for the hydrophobically-modified is consistent with expectations.[48] There is a significant monotonic increase in G' with the degree of substitution, resulting in a ~10-fold greater elasticity at 37 °C for the 6%-substituted alginate compared to the unmodified alginate. This suggests interactions between the side groups of the alginate chains which are contributing to increased viscoelasticity

in the polymer solution.[49,50] Fig. 2d shows temperature sweep tests for solutions of 1% w/v alginate with different degrees of substitution and 4% w/v MC. All solutions showed the formation of a thermo-gel with an apparent gelation temperature (T_g), defined as the temperature at which $G' > G''$, between 37–40 °C. Though the composite injectable formulation contains alginate microparticles suspended in a MC-containing buffer, we performed rheometry on MC-alginate solutions to investigate the effect of alginate on the gel structure of MC. We hypothesized that the composite hydrogel of alginate and MC would provide enhanced stability to the formation of the MC thermo-gel. All alginate-MC blends showed a ~3-fold increase in the gel strength at T_g compared to MC alone, and had higher G' and G'' values across the entire temperature range (Fig. 2d). Previous work on MC-alginate composites have proposed that the presence of alginate can synergistically promote the gelation of MC, leading to the formation of stronger and more thermoresponsive gels.[51–53] Our results are consistent with those found in the literature. These effects could be explained by hydrogen bonding and entanglement between the two polymers as well as the salting-out effect of the polyanionic alginate which dehydrates the MC network.[32,51,52] Hydrophobic interactions between MC and alginate have also been proposed, but there is a lack of high-quality data available.[53] Here, there were not significant differences between the blends with different degrees of alginate hydrophobicity at the tested conditions, which indicates that methylcellulose dominates the gel structure and mechanism. In addition, the thermoreversibility of methylcellulose was not affected by the addition of alginate, as discussed in the ESI (Fig. S5†).

The swelling ratio (Q_s) was also measured for blank (no ASD) alginate hydrogel particles synthesized *via* the centrifugal synthesis process described previously. Briefly, 2% w/v alginate solutions were prepared and passed through the microfluidic device in the centrifuge at 300 RCF. The particles were collected and weighed in their swollen and dried states to determine the swelling ratio, shown in Fig. 2e. The swelling ratio for hydrophobically-modified alginates is significantly lower compared to the unmodified alginate, with a ~2-fold decrease in Q_s for the 6%-d.s. alginate. The lower swelling ratios for the modified alginates correspond to the increase in elasticity of the respective polymer solutions, arising from hydrophobic associations between polymer chains. As swelling ratio is typically correlated with the mesh size of hydrogel networks, the decreased Q_s of the hydrophobically-modified alginate hydrogels indicate a tighter pore structure and slower free diffusion through the hydrogel which is beneficial for sustained release.

In vitro release studies

In this study, we used alginate microparticles, either unmodified or hydrophobically-modified, composited with MC polymer to form an injectable dual-network system for sustained release of the antibody drug. For a complete evaluation of the composite hydrogel system, the release profiles for multiple high-concentration solid antibody formulations with the composite system, alginate particles alone, MC hydrogels alone, pre-gels, and the ASD without any hydrogel are shown in Fig. 3. All *in vitro* release assays were performed with formulations with a C_{form} equivalent to 150 mg mL^{-1} and with 10% w/v PEG in the initial formulation to stabilize the ASD. The release profiles were fitted to the Weibull equation (eqn (3)), an empirical model for drug release kinetics from a hydrogel matrix.[54]

$$\frac{M_t}{M_\infty} = 1 - e^{-at^b} \tag{3}$$

where a and b are constants, with b corresponding to the mechanism of drug release. The value of b for each release profile was extracted to quantify the release behavior for different formulations. If $b \leq 0.75$, the mechanism is Fickian diffusion, reflecting first-order or burst release kinetics, and if $b > 1$, the mechanism is complex. Values of n between 0.75 and 1 correspond to anomalous transport of a combination between Fickian diffusion and polymer relaxation, which reflects the suppression of burst release and approaches zero-order kinetics as the value of b increases. Details of the model parameters and fits are available in Table S3 (ESI†).

For the formulations without methylcellulose (Fig. 3a and c), release of the antibody was achieved within minutes or hours. The ASD (solid antibody without hydrogel) and pre-gel (solid antibody with uncross-linked alginate) containing unmodified (0%-d.s.) alginate saw significant burst release within the first few minutes of the release test (Fig. 3a). In these cases, the extremely rapid drug release led to practically asymptotic profiles with unphysical values of the Weibull exponent ($b > 5$). The hydrogel particles containing unmodified (0%-d.s.) alginate also saw a burst release effect (Fig. 3c), which aligned with our previous results.[11] The formulations with hydrophobically-modified alginate had pronounced differences in the release profiles, even without MC. For the pre-gels, burst release was suppressed as the alginate's degree of substitution increased. The increasing hydrophobicity of the modified alginates contributes to slower water diffusion through the pre-gel and thus a slower dissolution of the solid antibody. We observe the same in the cross-linked alginate particles (Fig. 3c), where 100% of the total antibody was released from the unmodified particles within 1 hour, while only 44.7% and 17.2% of the antibody was released from the 3%-d.s. and 6%-d.s. particles in the same time, respectively. The release mechanism from the particles changed from first-order, diffusion-dominated kinetics for the unmodified particles ($b = 0.73$) to erosion-controlled transport for the particles with 6%-d.s. alginate ($b = 1.16$). The difference in release kinetics may be due to the reduced swelling behavior which was observed in the modified alginate particles, as well as interactions between IgG molecules and the hydrophobic side groups slowing transport of IgG.

Fig. 3b and d show the release profiles for the formulations with 4% w/v MC, either blended into the ASD or pre-gel (Fig. 3b) or in the suspension surrounding the hydrogel particles (Fig. 3d). In the case of the MC-containing formulations, release is achieved on the order of hours to days, a ~10-fold
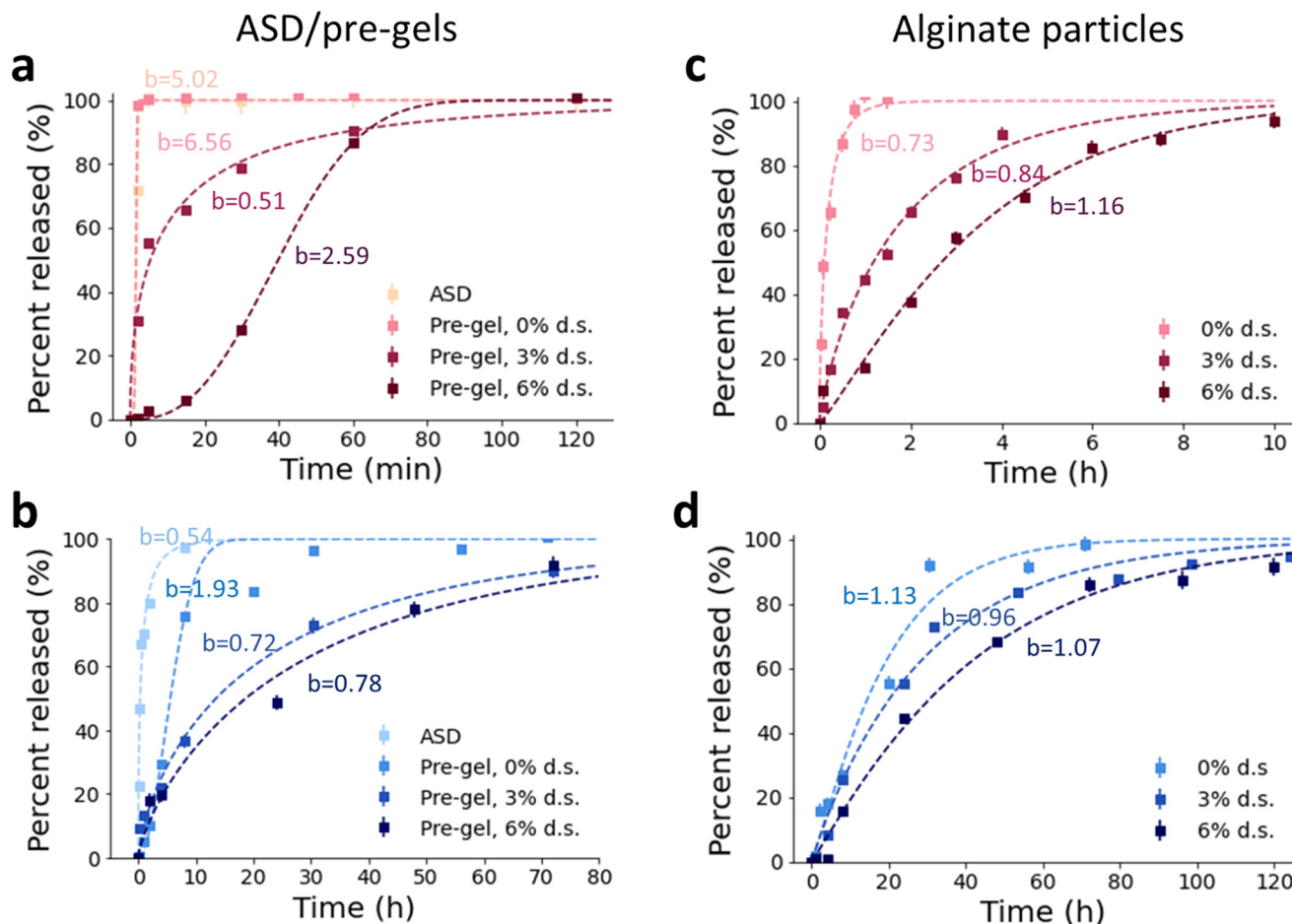
Fig. 3 Profiles of *in vitro* release tests performed in simulated bodily fluid, with dashed lines fitted to the Weibull model, for (a and b) ASD (amorphous solid antibody without alginate) and ASD pre-gel (solid antibody with 2% w/v uncross-linked alginate) formulations (a) without methylcellulose ($R^2 = 0.99-0.999$) and (b) with the addition of 4% w/v methylcellulose ($R^2 = 0.98-0.99$), and (c and d) ASD-laden alginate (2% w/v) microparticles (c) suspended in buffer ($R^2 = 0.99-0.991$) and (d) suspended in buffer with 4% w/v methylcellulose ($R^2 = 0.98-0.995$). The degree of alginate substitution was varied in the pre-gel and particle formulations. Data are shown for technical replicates, $n = 3$, and error bars show standard deviation.

increase in time scale compared to the formulations without MC. The difference in release time scale is due to formation of the thermo-gel depot upon injection into the release medium, a strategy that is widely used in drug delivery systems.[17,18,55,56] Burst release was significantly suppressed in these MC-containing formulations, with the pre-gels showing 5–13% and the particles showing <1–2% release of the total antibody within 1 hour. The ASDs and pre-gels showed primarily first-order release with $b = 0.54-0.78$ (Fig. 3b), indicating that diffusion through MC controls the release mechanism in this case, except for the 0% modified pre-gel, which has a sigmoidal release profile similar to those in Fig. 3a. When the alginate is cross-linked into particles (Fig. 3d), burst release is further suppressed and the release kinetics are in the range of erosion-controlled release ($b = 0.96-1.13$). The difference in the dominant release mechanism between the pre-gels and hydrogel particles indicates that the cross-linking of alginate contributes to slower diffusion and more linear release over time

in the composite system. The presence of the alginate network, in conjunction with MC, plays an important role in achieving sustained release without an initial burst. Additionally, inter-network penetration between the MC and alginate networks could result in adsorption of MC onto the particle, leading to slower diffusion of the drug through the pores of the alginate particle. In the case of the hydrophobically-modified alginates, interactions between the networks are enhanced, coupled with the lower water permeability and polymer–drug interactions of the hydrophobic alginate particles. These effects result in increasingly sustained release with the degree of alginate substitution, where we observed release over a few days ($t_{80} = 2.6$ days for 6%-d.s. particles in MC). This time scale of release indicates that the composite hydrogel system would be most effective for short-lived antibodies ($t_{1/2} < 7$ days), helping to extend the effective duration of the dosage and reduce the maximum serum concentration which is especially desirable for high-dose formulations.[22]

Compared to the alginate particles or MC hydrogel alone, the composite hydrogel showed sustained release, reduced burst release, and more erosion-controlled (zero-order) kinetics, which are desired features for drug delivery systems. To demonstrate that the control over release kinetics is consistent across several independent samples, *in vitro* release tests were replicated in multiple parallel samples ($n = 3$) for select formulations, which are shown in Fig. S6 (ESI†). The simultaneous high-loading and sustained-release capacities of the composite system is a unique feature, as typical hydrogels only achieve loadings of 0.01–1 mg mL^{-1} for biological molecules, and other 'high-loading' formulations do not exceed >100 mg mL^{-1} in antibody concentration.[14,45] Another advantage of this composite system is the ease of formulation by which diverse release profiles can be obtained, as the particles and the surrounding suspension media can be manipulated separately then blended together to yield the final formulation. For all formulations, complete or nearly complete (90–100%) release of antibody from the hydrogel was reached. For the particles where 100% release was not reached over the duration of the test, some amount of antibody could be entrapped within low-porosity regions of the hydrogel.[34,57,58]

Injectability studies

To assess injectability of the formulations, injection force tests were performed. Although material properties of the formulation such as viscosity and storage and loss modulus are important, they do not correlate directly to injectability for non-Newtonian solutions. Injection force is most clinically relevant measurement and the test yields quantitative results in a relatively simple manner.[59,60] A schematic for the injection force testing set-up is shown in Fig. 4a. The test was performed using a Zwick-Roell mechanical testing machine, equipped with a 500 N load cell and a custom 3D-printed attachment for compression of the syringe plunger. The hydrogel formulation was loaded into the syringe and an even downward force was applied onto the syringe plunger. An image of the injectability testing set-up is available in the ESI (Fig. S7†).

Fig. 4b and c show the injection force over the distance which was traveled by the plunger during the test at an injection rate of 25 µL s^{-1} ('slow' injection) and 150 µL s^{-1} ('fast' injection), respectively, for various formulation configurations. A higher injection rate is desirable for reducing the total duration of injection, but previous studies have found higher flow rates to be more painful, due to an increase in back pressure under the skin.[61–63] Therefore, these two injection rates were chosen to evaluate injectability at clinically relevant limits. All formulations tested had a C_{form} of 150 mg mL^{-1}. The tests were performed using a 24-gauge needle, which is within the range of needle bore sizes for subcutaneous injection.[64] The injection force for formulations with hydrogel particles are compared to the ASD and pre-gel formulations, and the formulation with particles were synthesized with unmodified alginate to provide a baseline for performance.

All the formulations tested had a maximum injection force (F_{max}) less than 10 N, which is well below the recommended acceptable maximum injection force for clinical use (20 N).[65] As observed in Fig. 4, each tested formulation experiences a 'start up' time at the beginning of the test where the injection force monotonically increases before reaching a plateau, at which the injection force can be averaged to yield the mean injection force ($\bar{F}$). We note here that the injection force profiles experience some variations across the distance travelled by the plunger, suggesting there are local differences in the distribution of the samples.[60] These variations are especially pronounced in the case of the alginate particles (either with or without methylcellulose), likely due to the reversible build-up and breakage of weak local structures as pressure is applied to the syringe plunger. At both tested flow rates, the pre-gels had a higher $\bar{F}$ than the ASDs alone, due to the alginate which makes the pre-gel more viscous. Notably, the pre-gels also had a higher $\bar{F}$ than the particles suspended only in 10% w/v PEG. In previous works, we hypothesized that antibody-loaded hydrogel particles would have improved flow behavior due to the spherical shape minimizing the surface area exposed for protein interactions, as well as the particles being soft and deformable even at high volume fractions.[11,34] The results here support our previous hypotheses and show that particle formulations have better injectability than equivalently-formulated pre-gels.
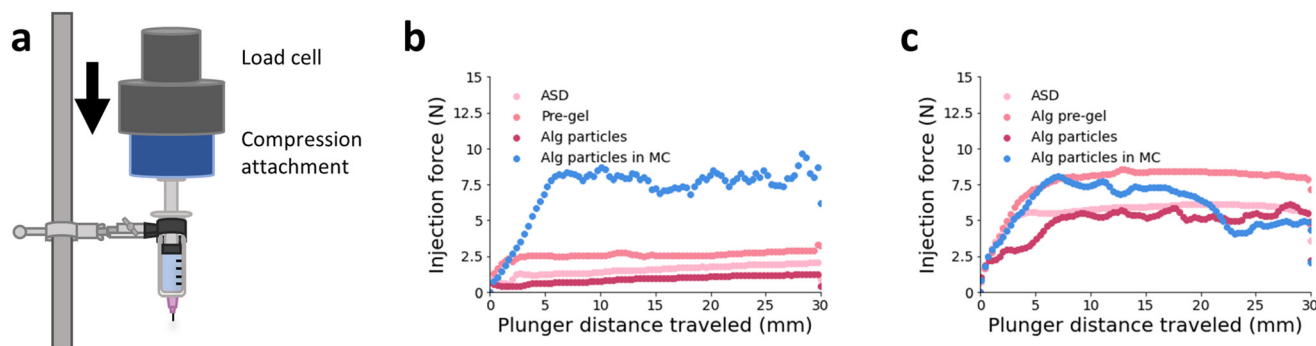

Fig. 4 (a) Schematic of injection force testing set-up. Injection force (N) *versus* distance traveled by syringe plunger (mm) for formulations tested at (b) 25 µL s^{-1} (~1.3 mm s^{-1}) and (c) 150 µL s^{-1} (~8.3 mm s^{-1}).

At the slow flow rate, the formulation for antibody-loaded particles suspended in 4% w/v methylcellulose had a significantly higher $\bar{F}$ than the other formulations, due to the viscosity of the methylcellulose (Fig. 4b). However, this difference in injectability is not observed at the higher flow rate. Theoretically, the Hagen–Poiseuille equation predicts that injection force should scale proportionally with the volumetric flow rate.[65] However, all formulations showed a less-than-proportional increase in injection force with the flow rate due to shear-thinning properties of the formulations. Particles suspended in 4% methylcellulose had a lower $\bar{F}$ at the high flow rate, indicating significant shear-thinning behavior due to the methylcellulose (Fig. 4c), although F_{max} is similar between the two flow rates. As discussed, the particles suspended in methylcellulose experience structural heterogeneities which result in 'bumpy' injection force profiles at both flow rates. At the slow flow rate, the longer residence time for the particles in the syringe could also contribute to the buildup of heterogeneous structures which explain the higher $\bar{F}$ compared to the fast flow rate. Overall, we show that the hydrogel particles maintain acceptable injectability properties, even when suspended in viscous polymer solutions.

Conclusions and future perspectives

In this work, we describe the formulation of injectable composite hydrogels consisting of alginate microparticles and thermoresponsive methylcellulose hydrogel for the delivery of high-concentration antibodies. The formulation process is relatively simple and modular as the synthesis of the microparticles and the composite hydrogel can be accomplished independently from each other. The alginate was modified with hydrophobic side groups to tune the release behavior of the particles, and alginate particles were prepared by gentle ionic cross-linking *via* centrifugal synthesis. We showed synergistic improvement of methylcellulose's thermoresponsive behavior with the addition of alginate, and *in vitro* release studies demonstrated that the composite system greatly suppresses burst release effect and sustains release of a model antibody drug, IgG, compared to the particles or methylcellulose hydrogel alone. We fitted the *in vitro* release profiles to the Weibull model, where the model parameter b was used to characterize the kinetics. We demonstrated a wide range of release kinetics (b = 0.73–1.16) for formulations with alginate microparticles with the ability to tune release based on the degree of alginate modification and the methylcellulose content. The composite system also showed acceptable injectability properties at clinically relevant testing conditions. Overall, the results suggest that the dual-network hydrogel composite system is a promising route to provide sustained- and controlled-release delivery of highly concentrated antibodies.

Due to the relative simplicity of formulation of the proposed system, we imagine the composite hydrogel to be used as an injectable depot-forming drug delivery system for controlling the release behavior of antibodies in a tunable manner. The proposed composite system also maintains the advantages of hydrogels in general for encapsulation and delivery of therapeutics, including its biocompatibility and stabilization of the antibody cargo in its solid form. In addition, the hydrogel's softness, deformability, and shear-thinning behavior enable ease of injection for highly concentrated dosage forms. Though we demonstrated this approach for formulating high-concentration amorphous solid antibodies, we also envision this to be a suitable concept for other physical states of the antibody, including crystalline solids and coacervates. Though IgG was used as a model drug in this study, given that the encapsulation approach is not specific to the therapeutic molecule and only relies the ability of the molecule to remain in a solid form, it is possible to expand this system to be a viable formulation platform for any therapeutic molecule in general, including small molecules, monoclonal antibodies, peptides, nucleic acids, and other advanced biologics. In moving towards clinical applications, however, several aspects must be addressed, such as evaluation of biocompatibility, cytotoxicity, and long-term stability of these formulations. Further characterization of *in vivo* bioavailability and pharmacokinetics for SC administration is also needed. Finally, because longer time scales of release may be desired for different clinical applications where the dose is ideally delivered over several weeks or months, additional consideration of polymer and hydrogel design to achieve greater extents of sustained release would be required. For example, different crosslinking chemistries can be incorporated in either the microparticle (*i.e.* Michael-type addition with functionalized alginate) or the thermo-gelling matrix (*i.e.* citric acid small molecule linker for methylcellulose hydrogels).

Author contributions

Talia Zheng: conceptualization, data curation, formal analysis, investigation, methodology, visualization, and writing (original draft). Patrick S. Doyle: conceptualization, funding acquisition, project administration, resources, supervision, validation, and writing (review & editing).

Data availability

No standardized datatype data were generated in this study. This study did not generate new code. Any additional information required to reanalyze the data reported in this paper is available from the corresponding author.

Conflicts of interest

Massachusetts Institute of Technology (MIT) has filed a provisional patent application on behalf of P. S. D. and T. Z. based on the research in this study.

Acknowledgements

References

1 G. J. Weiner, *Nat. Rev. Cancer*, 2015, **15**, 361–370.

2 C. Monaco, J. Nanchahal, P. Taylor and M. Feldmann, *Int. Immunol.*, 2015, **27**, 55–62.

3 I. Usach, R. Martinez, T. Festini and J.-E. Peris, *Adv. Ther.*, 2019, **36**, 2986–2996.

4 Z. Xu, J. H. Leu, Y. Xu, I. Nnane, S. G. Liva, S. X. Wang-Lin, R. Kudgus-Lokken, A. Vermeulen and D. Ouellet, *Clin. Pharmacol. Ther.*, 2023, **113**, 1011–1029.

5 W. Chen, B. C. Yung, Z. Qian and X. Chen, *Adv. Drug Delivery Rev.*, 2018, **127**, 20–34.

6 A. Erfani, A. E. Diaz and P. S. Doyle, *Mater. Today*, 2023, **65**, 227–243.

7 J. Liu, M. D. Nguyen, J. D. Andya and S. J. Shire, *J. Pharm. Sci.*, 2005, **94**, 1928–1940.

8 D. S. Tomar, S. Kumar, S. K. Singh, S. Goswami and L. Li, *mAbs*, 2016, **8**, 216–228.

9 J. Stevenson, R. Poker, J. Schoss, M. Campbell, C. Everitt, B. Holly, N. Stones, R. J. Pettis and M. Sanchez-Felix, *Adv. Drug Delivery Rev.*, 2024, **209**, 115322.

10 W. Jiskoot, A. Hawe, T. Menzen, D. B. Volkin and D. J. Crommelin, *J. Pharm. Sci.*, 2022, **111**, 861–867.

11 A. Erfani, P. Reichert, C. N. Narasimhan and P. S. Doyle, *iScience*, 2023, **26**, 107452.

12 J. Yoo and Y.-Y. Won, *ACS Biomater. Sci. Eng.*, 2020, **6**, 6053–6062.

13 X. Huang and C. S. Brazel, *J. Controlled Release*, 2001, **73**, 121–136.

14 J. Li, E. Weber, S. Guth-Gundel, M. Schuleit, A. Kuttler, C. Halleux, N. Accart, A. Doelemeyer, A. Basler, B. Tigani, K. Wuersch, M. Fornaro, M. Kneissel, A. Stafford, B. R. Freedman and D. J. Mooney, *Adv. Healthcare Mater.*, 2018, **7**, 1701393.

15 T. Nie, W. Wang, X. Liu, Y. Wang, K. Li, X. Song, J. Zhang, L. Yu and Z. He, *Biomacromolecules*, 2021, **22**, 2299–2324.

16 Y. Li, F. Wang and H. Cui, *Bioeng. Transl. Med.*, 2016, **1**, 306–322.

17 H. J. Moon, D. Y. Ko, M. H. Park, M. K. Joo and B. Jeong, *Chem. Soc. Rev.*, 2012, **41**, 4860–4883.

18 M. I. Rial-Hermida, A. Rey-Rico, B. Blanco-Fernandez, N. Carballo-Pedrares, E. M. Byrne and J. F. Mano, *ACS Biomater. Sci. Eng.*, 2021, **7**, 4102–4127.

19 H. Carrêlo, P. I. P. Soares, J. P. Borges and M. T. Cidade, *Gels*, 2021, **7**, 147.

20 L. Chen and S. A. Khan, *RSC Pharm.*, 2024, **1**, 689–704.

21 W. Liu, M. Griffith and F. Li, *J. Mater. Sci.: Mater. Med.*, 2008, **19**, 3365–3371.

22 C. M. Kasse, A. C. Yu, A. E. Powell, G. A. Roth, C. S. Liong, C. K. Jons, A. Buahin, C. L. Maikawa, X. Zhou, S. Youssef, J. E. Glanville and E. A. Appel, *Biomater. Sci.*, 2023, **11**, 2065–2079.

23 D. M. Nelson, Z. Ma, C. E. Leeson and W. R. Wagner, *J. Biomed. Mater. Res., Part A*, 2012, **100A**, 776–785.

24 C. R. Osswald and J. J. Kang-Mieler, *Ann. Biomed. Eng.*, 2015, **43**, 2609–2617.

25 J. Y. Chung, J. H. Ko, Y. J. Lee, H. S. Choi and Y.-H. Kim, *J. Controlled Release*, 2018, **276**, 42–49.

26 Y.-W. Won, J.-K. Kim, M.-J. Cha, K.-C. Hwang, D. Choi and Y.-H. Kim, *J. Controlled Release*, 2010, **144**, 181–189.

27 J. K. Kim, C. Yoo, Y.-H. Cha and Y.-H. Kim, *J. Controlled Release*, 2014, **194**, 316–322.

28 Y. Yang, W. Wu, H. Liu, H. Xu, Y. Zhong, L. Zhang, Z. Chen, X. Sui and Z. Mao, *J. Mol. Graphics Modell.*, 2020, **97**, 107554.

29 M. L. Coughlin, L. Liberman, S. P. Ertem, J. Edmund, F. S. Bates and T. P. Lodge, *Prog. Polym. Sci.*, 2021, **112**, 101324.

30 B. Niemczyk-Soczynska, P. Sajkiewicz and A. Gradys, *Polymers*, 2022, **14**, 1810.

31 H. Li, Y. J. Tan, K. F. Leong and L. Li, *ACS Appl. Mater. Interfaces*, 2017, **9**, 20086–20097.

32 H.-F. Liang, M.-H. Hong, R.-M. Ho, C.-K. Chung, Y.-H. Lin, C. H. Chen and H.-W. Sung, *Biomacromolecules*, 2004, **5**, 1917–1925.

33 E. Bulut, *Int. J. Biol. Macromol.*, 2021, **168**, 823–833.

34 A. Erfani, J. M. Schieferstein, P. Reichert, C. N. Narasimhan, C. Pastuskovas, V. Parab, D. Simmons, X. Yang, A. Shanker, P. Hammond and P. S. Doyle, *Adv. Healthcare Mater.*, 2022, 2202370.

35 H.-A. Kang, G.-J. Jeon, M.-Y. Lee and J.-W. Yang, *J. Chem. Technol. Biotechnol.*, 2002, **77**, 205–210.

36 H.-A. Kang, M. S. Shin and J.-W. Yang, *Polym. Bull.*, 2002, **47**, 429–435.

37 P. Laurienzo, M. Malinconico, A. Motta and A. Vicinanza, *Carbohydr. Polym.*, 2005, **62**, 274–282.

38 M. R. C. Marques, R. Loebenberg and M. Almukainzi, *Dissolution Technol.*, 2011, **18**, 15–28.

39 W. R. Strohl, *Antibody Ther.*, 2024, **7**, 132–156.

40 G. G. D'Ayala, M. Malinconico and P. Laurienzo, *Molecules*, 2008, **13**, 2069–2106.

41 S. R. Banks, K. Enck, M. Wright, E. C. Opara and M. E. Welker, *J. Agric. Food Chem.*, 2019, **67**, 10481–10488.

42 S. Akshaya and A. J. Nathanael, *ACS Omega*, 2024, **9**(4), 4246–4262.

43 S. K. Bharti and R. Roy, *TrAC, Trends Anal. Chem.*, 2012, **35**, 5–26.

44 A. Nochos, D. Douroumis and N. Bouropoulos, *Carbohydr. Polym.*, 2008, **74**, 451–457.

45 M. D. Baumann, C. E. Kang, J. C. Stanwick, Y. Wang, H. Kim, Y. Lapitsky and M. S. Shoichet, *J. Controlled Release*, 2009, **138**, 205–213.

46 S. Marquette, C. Peerboom, A. Yates, L. Denis, J. Goole and K. Amighi, *Eur. J. Pharm. Biopharm.*, 2014, **86**, 393–403.

47 P. Zhai, X. B. Chen and D. J. Schreyer, *Mater. Sci. Eng., C*, 2015, **56**, 251–259.

48 D. Chandler, *Nature*, 2005, **437**, 640–647.

49 K. C. Tam and C. Tiu, *J. Rheol.*, 1989, **33**, 257–280.

50 J. Wang, L. Shi, S. Zhu, Y. Xiong and Q. Liu, *AIP Adv.*, 2021, **11**, 065324.

51 P. Kumar and Y. E. Choonara, *Mater. Res. Express*, 2021, **8**, 105303.

52 T. Shimoyama, K. Itoh, M. Kobayashi, S. Miyazaki, A. D'Emanuele and D. Attwood, *Drug Dev. Ind. Pharm.*, 2012, **38**, 952–960.

53 O. Eskens, G. Villani and S. Amin, *Cosmetics*, 2021, **8**, 3.

54 V. Papadopoulou, K. Kosmidis, M. Vlachou and P. Macheras, *Int. J. Pharm.*, 2006, **309**, 44–50.

55 R. Fan, Y. Cheng, R. Wang, T. Zhang, H. Zhang, J. Li, S. Song and A. Zheng, *Polymers*, 2022, **14**, 2379.

56 M. Norouzi, B. Nazari and D. W. Miller, *Drug Discovery Today*, 2016, **21**, 1835–1849.

57 A. Bertz, S. Wöhl-Bruhn, S. Miethe, B. Tiersch, J. Koetz, M. Hust, H. Bunjes and H. Menzel, *J. Biotechnol.*, 2013, **163**, 243–249.

58 G. Jahanmir, C. M. L. Lau, M. J. Abdekhodaie and Y. Chau, *ACS Appl. Bio Mater.*, 2020, **3**, 4208–4219.

59 T. E. Robinson, E. A. B. Hughes, N. M. Eisenstein, L. M. Grover and S. C. Cox, *J. Visualized Exp.*, 2020, e61417.

60 M. H. Chen, L. L. Wang, J. J. Chung, Y.-H. Kim, P. Atluri and J. A. Burdick, *ACS Biomater. Sci. Eng.*, 2017, **3**, 3146–3160.

61 D. V. Doughty, C. Z. Clawson, W. Lambert and J. A. Subramony, *J. Pharm. Sci.*, 2016, **105**, 2105–2113.

62 C. Patte, S. Pleus, C. Wiegel, G. Schiltges, N. Jendrike, C. Haug and G. Freckmann, *Diabetes Technol. Ther.*, 2013, **15**, 289–294.

63 J. Gupta, S. S. Park, B. Bondy, E. I. Felner and M. R. Prausnitz, *Biomaterials*, 2011, **32**, 6823–6831.

64 *Vaccine Administration: General Best Practices for Immunization*, **https://www.cdc.gov/vaccines/hcp/acip-recs/general-recs/administration.html**.

65 R. P. Watt, H. Khatri and A. R. Dibble, *Int. J. Pharm.*, 2019, **554**, 376–386.